

Thermodynamics of a d -wave Superconductor Near a Surface

L.J. Buchholtz

Department of Physics, California State University, Chico, Chico, CA 95929, USA

Mario Palumbo, D. Rainer

Physikalisches Institut, Universität Bayreuth, D-95440 Bayreuth, Germany

J.A. Sauls

Department of Physics & Astronomy, Northwestern University, Evanston, IL 60208, USA

Abstract

We study the properties of an anisotropically paired superconductor in the presence of a specularly reflecting surface. The bulk stable phase of the superconducting order parameter is taken to have $d_{x^2-y^2}$ symmetry. Contributions by order parameter components of different symmetries vanish in the bulk, but may enter in the vicinity of a wall. We calculate the self-consistent order parameter and surface free energy within the quasiclassical formulation of superconductivity. We discuss, in particular, the dependence of these quantities on the degree of order parameter mixing and the surface to lattice orientation. Knowledge of the thermodynamically stable order parameter near a surface is a necessary precondition for calculating measurable surface properties which we present in a companion paper.

To appear in J. Low Temp. Phys., Vol. 101, Dec., 1995

I. INTRODUCTION

Anisotropic superconductors react sensitively to electron scattering from impurities, interfaces and surfaces [1]. Scattering leads, in these cases, to pair-breaking and a modification of the superconducting state. This paper is a first step in a systematic study of the effects of surface scattering on the superconducting properties of a layered system with d -wave pairing. The possibility of d -wave pairing is currently under serious consideration as a promising candidate for the proper order parameter symmetry in the high- T_c cuprates [2–8]. The presence of a d -wave pairing interaction results in a strongly anisotropic superconducting order parameter, and one expects that surfaces will exert a sizable influence on the pair condensate near the boundary [1,9–20]. Correspondingly, the physical properties of a d -wave system near an interface may be profoundly different from those of an s -wave superconductor. The distinction is primarily due to the strongly enhanced pair-breaking effects in a d -wave system. Many standard experiments, such as tunneling measurements or electromagnetic absorption at surfaces (in the very long mean free path limit), are particularly sensitive to the superconducting state near the interface. This suggests that experiments directed at measuring effects deriving from the interaction of the superconducting order parameter with a surface or interface may serve as reliable probes for the symmetry of the superconducting order parameter. The optimal surfaces for studying d -wave symmetry are those oriented perpendicular to the layers, and we consider this geometry exclusively here.

Because the superconducting order parameter is itself not directly accessible to experiments, any evidence for an unconventional symmetry of the order parameter must be more or less indirect. Theory is required to extract information on the order parameter from the experimental properties of the superconductor, and to point out measurable effects which reflect clearly the symmetry of the underlying order parameter. This paper and the companion paper, [II] [21], discuss specific aspects of anisotropic superconductivity near surfaces. We consider systems with tetragonal (D_{4h}) crystal symmetry, which is a good *approximate* symmetry of the cuprate superconductors, and focus on a non-degenerate order parameter (Cooper pair wavefunction) of even parity. A group theoretical classification of superconducting order [22] leads, in this case, to four different types of bulk order parameters corresponding to the four one-dimensional, even parity representations of the D_{4h} group: the A_1 , or identity representation, the A_2 representation, and the B_1 and B_2 representations. Whichever representation leads to the largest attractive coupling constant for Cooper pairs will determine the symmetry and transition temperature of the bulk superconducting state. A surface, on the other hand, may break the D_{4h} symmetry and thus may admit local contributions from all

other representations, to a degree depending on the magnitude of their coupling constants. In addition, surface pair-breaking may suppress the dominant bulk order parameter and generate surface states of a new symmetry. Surface pair-breaking and the mixing in of new symmetries thus leads to measurable modifications of the superconducting properties near a surface, which carry information on the symmetry of the superconducting order parameter.

We investigate both the thermodynamic and spectral properties of a superconductor in the vicinity of a specular interface. We first focus on calculations of the spatial dependence of the order parameter (gap function) and of the surface free energy as functions of the relative surface to crystal lattice orientation. We take the bulk order parameter to be of B_1 d -wave symmetry as predicted by microscopic models [2,3], and indicated by various experiments. In the presence of a surface, we consider three main order parameter categories: those possessing a single B_1 d -wave component (all other coupling constants being assumed negligible), those possessing a linear combination of B_1 and B_2 d -wave components (the A_1 and A_2 coupling constants being assumed negligible), and those possessing a linear combination of the A_1 , A_2 , B_1 , and B_2 components (i.e. all components allowed by symmetry may couple in). We discuss to what extent the mixing of these various symmetry components affects the overall order parameter structure in the vicinity of a surface as well as the corresponding effect on the surface free energy. We use these results in [II] to study the influence of surface pair-breaking on the tunneling density of states.

We perform all of our calculations within the quasiclassical formulation of superconductivity. This is a fully self-consistent theory which requires the numerical calculation of the quasiclassical propagator from which the thermodynamic and spectral data may then be extracted. The formulation is justified as long as the superconducting coherence length is large compared to the Fermi wavelength. This approximation is known to be excellent for traditional superconductors, but it may be of reduced validity for the high- T_c cuprates due to their substantially shorter coherence lengths. In section II we give a brief review of the quasiclassical framework, and in section III we present our numerical results for the gap-function and free energy. A discussion and summary are contained in section IV.

II. QUASICLASSICAL THEORY

The quasiclassical formulation of superconductivity was first stated by Eilenberger [23], Larkin and Ovchinnikov [24,25], and Eliashberg [26]. This theory is capable of describing both the equilibrium and dynamical properties of conduction electrons in either the normal or superconducting state and may be understood as a generalization of Landau's theory of normal Fermi liquids. In this section we give a brief summary of only those equations relevant to the current analysis. Readers interested in a more detailed presentation are referred to the original papers mentioned above, and to the recent review articles [27–30]. As our primary resource regarding the quasiclassical formulation we turn to reference [28], whose notation we adopt whenever possible.

In this paper we present calculations of the *thermodynamic* properties of a superconducting system in equilibrium and, correspondingly, require only the quasiclassical theory in its imaginary-energy (Matsubara) representation. The fundamental quantity in the quasiclassical formulation is the matrix propagator for quasiparticle excitations, \hat{g} . For spin-independent systems the propagator has the simple form:

$$\hat{g}(\mathbf{p}_f, \mathbf{R}; \epsilon_n) = \begin{pmatrix} g & f \\ \bar{f} & \bar{g} \end{pmatrix}, \quad (1)$$

which is a 2×2 matrix in particle-hole (Nambu) space. The propagator \hat{g} is a function of a momentum on the Fermi surface, \mathbf{p}_f , a real-space position, \mathbf{R} , and an imaginary excitation energy, $i\epsilon_n$. The diagonal components of \hat{g} carry information on the spectrum of Bogoliubov quasiparticles, while the off-diagonal components are related to the Cooper pair amplitude. The functions \bar{f} and \bar{g} are related to f and g by fundamental symmetry identities [28].

The central equation obeyed by the propagator \hat{g} is the quasiclassical transport equation

$$\left[i\epsilon_n \hat{\tau}_3 - \hat{\Delta}(\mathbf{p}_f, \mathbf{R}), \hat{g}(\mathbf{p}_f, \mathbf{R}; \epsilon_n) \right] + i\mathbf{v}_f(\mathbf{p}_f) \cdot \vec{\nabla}_{\mathbf{R}} \hat{g}(\mathbf{p}_f, \mathbf{R}; \epsilon_n) = 0, \quad (2)$$

supplemented by a normalization condition

$$[\hat{g}(\mathbf{p}_f, \mathbf{R}; \epsilon_n)]^2 = -\pi^2 \hat{1}. \quad (3)$$

The pairing self-energy¹ $\hat{\Delta}$ is computed, within the weak coupling approximation, from the self-consistency equation:

¹Note that we are using the terms pairing self-energy, order parameter, and gap function interchangeably.

$$\hat{\Delta}(\mathbf{p}_f, \mathbf{R}) = T \sum_{\epsilon_n}^{\epsilon_{co}} \oint d\mathbf{p}'_f n(\mathbf{p}'_f) V(\mathbf{p}_f, \mathbf{p}'_f) \hat{f}(\mathbf{p}'_f, \mathbf{R}; \epsilon_n). \quad (4)$$

Here $V(\mathbf{p}_f, \mathbf{p}'_f)$ is the pairing interaction, which determines both T_c and the symmetry of the order parameter, and $\hat{f}(\mathbf{p}_f, \mathbf{R}; \epsilon_n)$ is the off-diagonal part of the full matrix propagator $\hat{g}(\mathbf{p}_f, \mathbf{R}; \epsilon_n)$. The integration over \mathbf{p}_f is to be interpreted as a normalized Fermi surface integral such that $\oint d\mathbf{p}_f n(\mathbf{p}_f) = 1$, where $n(\mathbf{p}_f)$ is the Fermi surface anisotropy factor (see [II]). Equations (2) and (4) must be solved self-consistently for the position dependent gap function $\hat{\Delta}(\mathbf{p}_f, \mathbf{R})$.

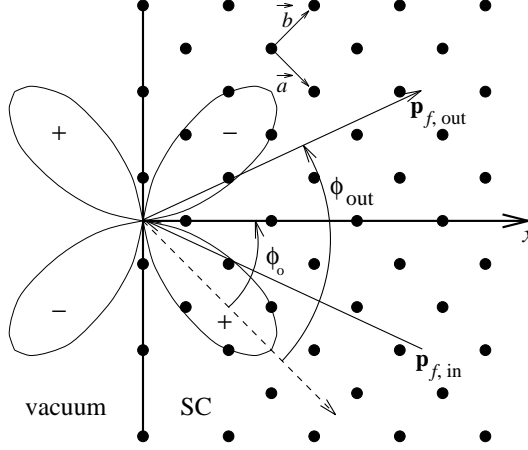


Fig. 1. This figure defines the geometrical configuration and the central descriptive parameters of our calculation. We sketch the clover-shaped B_1 d -wave gap structure whose bulk orientation is fixed to the crystal lattice. The angle ϕ_o is the surface to lattice orientation angle ($\phi_o = 45$ deg in this case), while ϕ_{out} defines the trajectory of the out-going quasiparticle. The trajectory of the incoming quasiparticle is specified by $(\phi_{\text{in}} - \phi_o) = \pi - (\phi_{\text{out}} - \phi_o)$.

We consider a semi-infinite system occupying the space $x > 0$ with a single specularly reflecting interface located at $x = 0$; this configuration is depicted in Fig. 1. The boundary condition for the quasiclassical propagator \hat{g} at a specular wall requires continuity along a reflected trajectory: [28]

$$\hat{g}(\mathbf{p}_{f,\text{in}}, \mathbf{R}_{\text{wall}}; \epsilon_n) = \hat{g}(\mathbf{p}_{f,\text{out}}, \mathbf{R}_{\text{wall}}; \epsilon_n), \quad (5)$$

where the out-going momentum vector, $\mathbf{p}_{f,\text{out}}$, is given in terms of the in-coming momentum vector, $\mathbf{p}_{f,\text{in}}$, and the surface normal, \hat{n} , by

$$\mathbf{p}_{f,\text{out}} = \mathbf{p}_{f,\text{in}} - 2\hat{n}(\hat{n} \cdot \mathbf{p}_{f,\text{in}}). \quad (6)$$

Note that an anisotropic order parameter need not, in general, be continuous at the surface along a given trajectory since the momentum vector abruptly changes direction there.

In our model we assume a homogeneous order parameter in the plane of the surface; in this way there is only one relevant spatial degree of freedom which allows us, in the following, to replace \mathbf{R} by x . Further, we consider layered superconductors with negligibly small interlayer coupling. We model these systems by a cylindrical Fermi surface with no dependence of the gap function on p_z so that the Fermi surface vector \mathbf{p}_f can be replaced simply by the azimuthal angle ϕ . These simplifications allow us to rewrite the quasiclassical transport equation in the form

$$\left[i\epsilon_n \hat{\tau}_3 - \hat{\Delta}(\phi, x), \hat{g}(\phi, x; \epsilon_n) \right] + iv_f \cos \phi \frac{\partial}{\partial x} \hat{g}(\phi, x; \epsilon_n) = 0, \quad (7)$$

which amounts to an ordinary first order differential equation along a given “trajectory” (incoming and outgoing) which is defined by the parameter ϕ . These trajectories may be understood as “classical” trajectories of particles moving with velocity v_f along the direction ϕ and being reflected at the surface. A typical trajectory is shown in Fig. 1 where we have chosen to measure the angle ϕ relative to the crystal \hat{a} -axis. In our simplified model the Fermi surface parameters are assumed isotropic in the ab -plane, and the reduction to tetragonal symmetry comes about only

via the pairing interaction. The use of more general Fermi surface parameters would not alter the main results of our calculations.¹

We incorporate contributions to the pairing self-energy from the A_1 , A_2 , B_1 , and B_2 representations of the tetragonal group. Our approximate order parameter is taken to be a linear combination of simple trigonometric functions of the angle ϕ :²

$$\begin{aligned}\hat{\Delta}(\phi, x) &= \hat{\Delta}_s(\phi, x) + \hat{\Delta}_{g_1}(\phi, x) + \hat{\Delta}_{g_2}(\phi, x) + \hat{\Delta}_{d_1}(\phi, x) + \hat{\Delta}_{d_2}(\phi, x) \\ &= \hat{\Delta}_s(x) \times 1 + \hat{\Delta}_{g_1}(x) \times \cos 4\phi + \hat{\Delta}_{g_2}(x) \times \sin 4\phi \\ &\quad + \hat{\Delta}_{d_1}(x) \times \cos 2\phi + \hat{\Delta}_{d_2}(x) \times \sin 2\phi\end{aligned}\tag{8}$$

In the usual notation, 1 is an s -wave function, $\cos 4\phi$ and $\sin 4\phi$ are g -wave functions of A_1 and A_2 symmetry respectively, and $\cos 2\phi$ and $\sin 2\phi$ are d -wave functions of B_1 and B_2 symmetry. In accordance with equation (8), we decompose the gap equation (4) into the following five self-consistency equations:

$$\hat{\Delta}_s(x) = V_s T \sum_{\epsilon_n}^{\epsilon_{co}} \oint \frac{d\phi'}{2\pi} \hat{f}(\phi', x; \epsilon_n),\tag{9}$$

$$\hat{\Delta}_{g_1}(\phi, x) = V_{g_1} T \sum_{\epsilon_n}^{\epsilon_{co}} \oint \frac{d\phi'}{2\pi} 2 \cos 4\phi \cos 4\phi' \hat{f}(\phi', x; \epsilon_n),\tag{10}$$

$$\hat{\Delta}_{g_2}(\phi, x) = V_{g_2} T \sum_{\epsilon_n}^{\epsilon_{co}} \oint \frac{d\phi'}{2\pi} 2 \sin 4\phi \sin 4\phi' \hat{f}(\phi', x; \epsilon_n),\tag{11}$$

$$\hat{\Delta}_{d_1}(\phi, x) = V_{d_1} T \sum_{\epsilon_n}^{\epsilon_{co}} \oint \frac{d\phi'}{2\pi} 2 \cos 2\phi \cos 2\phi' \hat{f}(\phi', x; \epsilon_n),\tag{12}$$

$$\hat{\Delta}_{d_2}(\phi, x) = V_{d_2} T \sum_{\epsilon_n}^{\epsilon_{co}} \oint \frac{d\phi'}{2\pi} 2 \sin 2\phi \sin 2\phi' \hat{f}(\phi', x; \epsilon_n).\tag{13}$$

where the V_X are coupling constants, and the indices s , d , and g refer to s -wave, d -wave, and g -wave respectively. Note that $\hat{\Delta}_s(\phi, x)$ and $\hat{\Delta}_{g_1}(\phi, x)$ have A_1 symmetry, $\hat{\Delta}_{g_2}(\phi, x)$ has A_2 symmetry, and $\hat{\Delta}_{d_1}(\phi, x)$ and $\hat{\Delta}_{d_2}(\phi, x)$ have B_1 and B_2 symmetry respectively. One can always eliminate the coupling constants V_X , along with the frequency-sum cutoffs ϵ_{co} , in favor of the transition temperatures via the customary BCS relation $T_{cX} \sim 1.13\epsilon_{co}e^{-1/V_X}$, where X denotes the subscripts s , g_1 , g_2 , d_1 , and d_2 . In general, V_X may be positive (attractive) or negative (repulsive).

Equations (7)–(13) must be solved self-consistently for the spatially dependent gap amplitudes, $\Delta_X(x)$, which are the upper right elements of the corresponding pairing self-energies,

$$\hat{\Delta}_X(x) = \begin{pmatrix} 0 & \Delta_X(x) \\ -\Delta_X(x) & 0 \end{pmatrix}.\tag{14}$$

We may then proceed to calculate various thermodynamic quantities such as the free energy difference per unit surface area:

$$\Omega_{\text{surf}} = \int_0^\infty dx \{ \mathcal{F}(x) - \mathcal{F}_{\text{bulk}} \},\tag{15}$$

where $\mathcal{F}(x)$ is the free energy density in the presence of the wall,

$$\mathcal{F}(x) = N(E_F) \left\{ \ln \left(\frac{T}{T_{cs}} \right) |\Delta_s(x)|^2 + \frac{1}{2} \left[\ln \left(\frac{T}{T_{cg_1}} \right) |\Delta_{g_1}(x)|^2 + \ln \left(\frac{T}{T_{cg_2}} \right) |\Delta_{g_2}(x)|^2 \right] \right\}$$

¹A significant influence of the Fermi surface geometry is expected if the Fermi energy lies near a Van Hove singularity (for a discussion of these topics see Refs. [31–34]). The effect of non-trivial Fermi surfaces will be discussed in a future publication.

²The precise ϕ -dependence of the order parameter is still controversial [35]. For this study we decided to parameterize the ϕ dependence in a straight forward way. An alternative approach would have been to take the order parameter from calculations in the single-exchange graph approximation. [36].

$$\begin{aligned}
& + \ln \left(\frac{T}{T_{cd_1}} \right) |\Delta_{d_1}(x)|^2 + \ln \left(\frac{T}{T_{cd_2}} \right) |\Delta_{d_2}(x)|^2 \Big\} \\
& + iN(E_F)k_B T \sum_{\epsilon_n > 0} \int_{\epsilon_n}^{\infty} d\lambda \int \frac{d\phi}{2\pi} \left(\text{tr}_4 [\hat{\tau}_3 (\hat{g}(\phi, x; \lambda) - \hat{g}_0(\phi; \lambda))] - 2i \frac{\pi |\Delta(\phi, x)|^2}{\lambda^2} \right). \tag{16}
\end{aligned}$$

and \mathcal{F}_{bulk} is obtained by setting $\Delta(\phi, x) = \Delta_{bulk}(\phi)$. Here \hat{g}_0 is the normal state propagator, and $\Delta(\phi, x)$ is the full, ϕ -dependent gap amplitude. In the next section we make use of the preceding equations to calculate the various gap amplitudes and the surface free energy for various surface orientations.

III. RESULTS

We consider a superconductor-insulator interface, with the superconductor occupying the space $x > 0$. We compute the constituent quantities as a function of x out to a distance of $\sim 30\xi$ ($\xi = \hbar v_f / \pi \Delta_{max}(x = \infty)$) from the wall. We consider an ideal interface by imposing a specular boundary condition at the wall, which amounts to the condition:

$$\hat{g}(\phi_{in}, x = 0; \epsilon_n) = \hat{g}(\phi_{out}, x = 0; \epsilon_n), \tag{17}$$

where ϕ_{out} is the complementary angle to ϕ_{in} (obtained upon specular reflection of the trajectory) and is given by $(\phi_{out} - \phi_o) = \pi - (\phi_{in} - \phi_o)$.

We divide the presentation of our results into two subsections. In the first subsection we consider a simple d -wave order parameter of the form $\Delta(\phi, x) = \Delta_{d_1}(x) \cos 2\phi$, and in the second we include the possibility of admixtures of components of different symmetries which are induced by the interaction with the surface.

A. Simple d -wave Model

In this section we consider a pairing interaction of the form $V(\phi, \phi') = 2V_{d_1} \cos 2\phi \cos 2\phi'$, which corresponds to a purely d -wave order parameter of B_1 symmetry. This is the symmetry favored by microscopic theories to give the highest T_c [2,3]. The order parameter has the form: $\hat{\Delta}(\phi, x) = \hat{\Delta}_{d_1}(x) \cos 2\phi$ where $\hat{\Delta}_{d_1}(x)$ must be evaluated self-consistently from equations (7) and (12). In Fig. 2 we plot the gap amplitude $\Delta_{d_1}(x)$ as a function of x for various surface to lattice orientation angles ϕ_o (the angle ϕ_o is defined in Fig. 1). Note that for an orientation angle $\phi_o = 0$ the gap amplitude is not suppressed by the presence of the wall. This is analogous to the isotropic s -wave case. However as the surface to lattice orientation angle increases the gap amplitude rapidly becomes suppressed in the vicinity of the wall and it completely vanishes at the wall for $\phi_o = 45$ deg. Note that this suppression heals on the scale of about six coherence lengths.

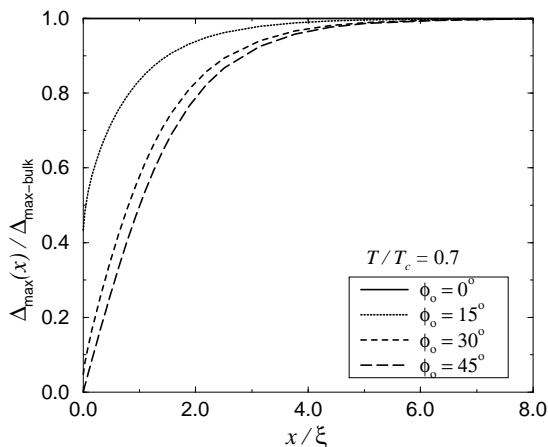


Fig. 2 The order parameter amplitude as a function of position when only one d -wave component is present, for various surface to lattice orientation angles, ϕ_o .

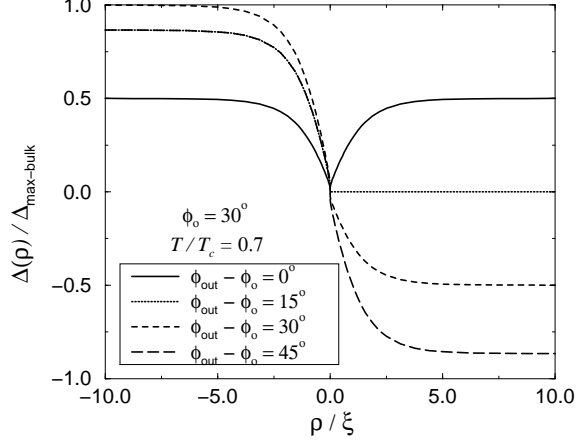


Fig. 3 The local order parameter experienced by a quasiparticle moving along a trajectory with angle ϕ_{out} for a surface to lattice orientation angle of $\phi_o = 30$ deg. The parameter ρ is the coordinate position *along* the trajectory and is related to x via $\rho = x / \cos \phi_{\text{out}} - \phi_o$. The point of reflection is taken to be $\rho = 0$.

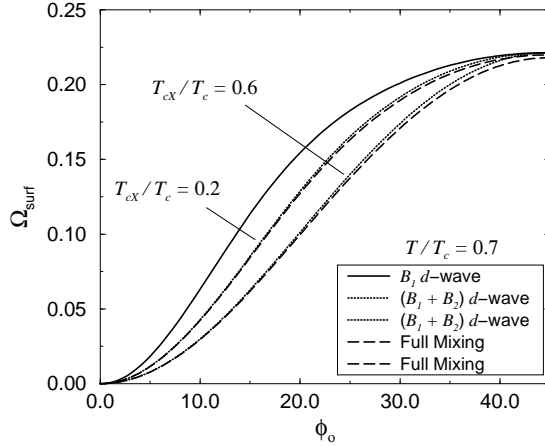


Fig. 4 The surface free energy as a function of surface to lattice orientation, ϕ_o , for various degrees of mixing in units of $(N(E_F)|\Delta_{\text{max-bulk}}(T=0)|^2\xi)$. The two center lines correspond to the low transition temperature regime ($T_{cX}/T_c = 0.2$) while the lower two lines correspond to the high transition temperature regime ($T_{cX}/T_c = 0.6$). The solid line corresponds to purely B_1 pairing.

The angular dependence of the total gap suppression can be understood within the framework of the quasiclassical approximation. A quasiparticle moving along a classical trajectory experiences the local order parameter with momentum along ϕ (i.e. in the direction of the trajectory). For a surface parallel to one of the crystal axes, the local order parameter is constant along the trajectory because $\hat{\Delta}_{d_1}(\phi_{\text{in}}) = \hat{\Delta}_{d_1}(\phi_{\text{out}})$ and the solution of the transport equation along this trajectory is identical to the corresponding solution in the bulk. As a consequence, the self-consistently determined order parameter is identical to the bulk order parameter for this orientation of the surface and the surface free energy is zero. For any other surface orientation one has $\hat{\Delta}_{d_1}(\phi_{\text{in}}) \neq \hat{\Delta}_{d_1}(\phi_{\text{out}})$, and the propagator \hat{f} , and consequently the self-consistent order parameter, will be modified by the surface. In Fig. 3 we plot the local order parameter Δ as a function of the spatial position, ρ , *along* the trajectory for a surface orientation $\phi_o = 30$ deg and several different trajectories. The point of reflection is taken to be at $\rho = 0$, with negative ρ values denoting an incoming particle. This depicts the local gap amplitude that a quasiparticle experiences along its trajectory. As

previously mentioned, a discontinuous jump in the order parameter upon reflection at the wall can be observed along all trajectories (except when $\phi_{\text{out}} - \phi_o = 0$ deg) due to the discontinuous change in momentum direction. Parenthetically, we note that an asymptotic change in sign of the order parameter along a trajectory (e.g. Fig. 3, trajectories $\phi_{\text{out}} - \phi_o = 30$ deg and 45 deg) can give rise to significant spectral effects such as zero-energy bound states [37] and Tomasch oscillations [11]. Our discussion of spectral effects will appear in a companion paper.

The surface free energy for the case of a simple d -wave order parameter is displayed as a function of the surface orientation angle ϕ_o in Fig. 4 as the solid line. The surface energy is zero, as expected, for a surface parallel to one of the crystal axes ($\phi_o = 0$ deg, 90 deg, ...). For any other orientation the surface energy is positive as a consequence of the surface pair-breaking. Observe, in this case, that the energy values are very strongly dependent on the relative orientation of the gap nodes with respect to the wall. These qualitative features of the pure d -wave model will persist even if components of other symmetries are mixed in. However, as we discuss in the following subsection, mixing in leads to significant quantitative differences in the order parameter structure and the surface free energy.

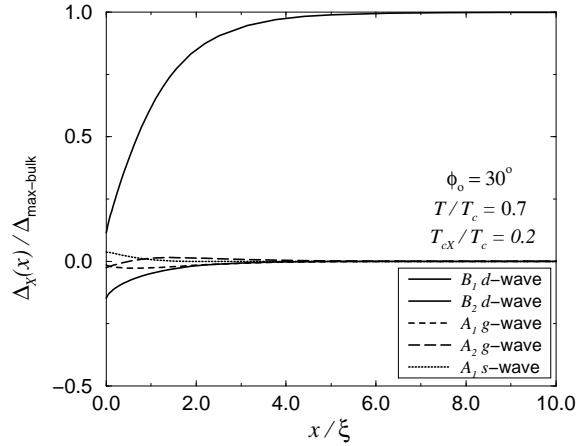


Fig. 5 The individual gap amplitudes, $\Delta_X(x)$, as functions of x for the low coupling constant regime ($T_{cX}/T_c = 0.2$) at a surface to lattice orientation angle of $\phi_o = 30$ deg.

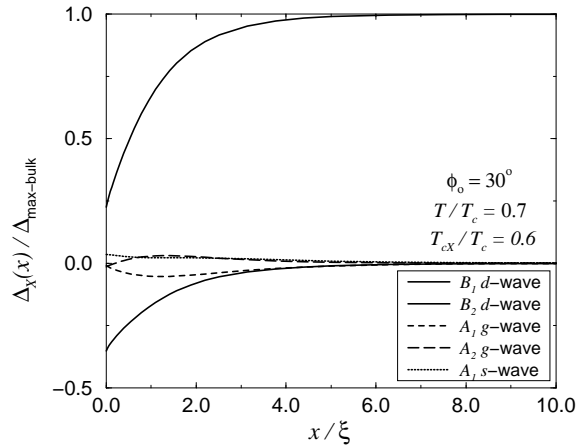


Fig. 6 The individual gap amplitudes, $\Delta_X(x)$, as functions of x for the low coupling constant regime ($T_{cX}/T_c = 0.6$) at a surface to lattice orientation angle of $\phi_o = 30$ deg.

B. Extended d -wave Model

In this section we consider an admixture of the previously mentioned components Δ_s , Δ_{d_2} , Δ_{g_1} , and Δ_{g_2} to the dominant Δ_{d_1} component. Thus the total gap amplitude has the form

$$\begin{aligned} \Delta(\phi, x) = & \Delta_s(x) + \Delta_{g_1}(x) \cos 4\phi + \Delta_{g_2}(x) \sin 4\phi \\ & + \Delta_{d_1}(x) \cos 2\phi + \Delta_{d_2}(x) \sin 2\phi. \end{aligned} \quad (18)$$

The degree to which a component Δ_X mixes in is determined by the corresponding transition temperature, T_{cX} . The dominant component has the highest transition temperature (T_{cd_1}) and provides the scale for all other temperatures in the calculation. Accordingly, we have $T_c \equiv T_{cd_1}$ and then the ratios T_{cX}/T_c become the parameters of the calculation. We consider only coupling constant and temperature values for which the non-dominant components (i.e. $T_{cX}/T_c < 1$) vanish in the bulk, but may appear near the wall. The admixture of the subordinate components changes the momentum dependence of the gap function. For instance, an admixture of Δ_{d_2} causes a rotation of the total gap (e.g. Δ_{d_2} alone is equivalent to a 45 deg rotation in momentum space). The effective gap maximum and the angular position of the gap's nodes thus vary, in general, with distance from the wall. By means of mixing in the new components, the system is able to alter the gap's angular and spatial structure and thereby further lower its free energy.

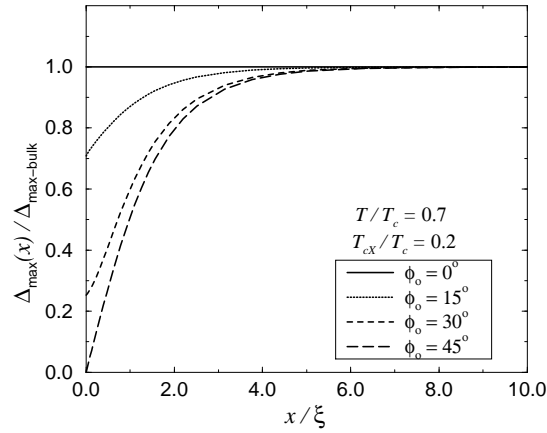


Fig. 7 The maximum of the total order parameter as a function of x in the low coupling constant regime, $T_{cX}/T_c = 0.2$, for various surface to lattice orientation angles, ϕ_o .

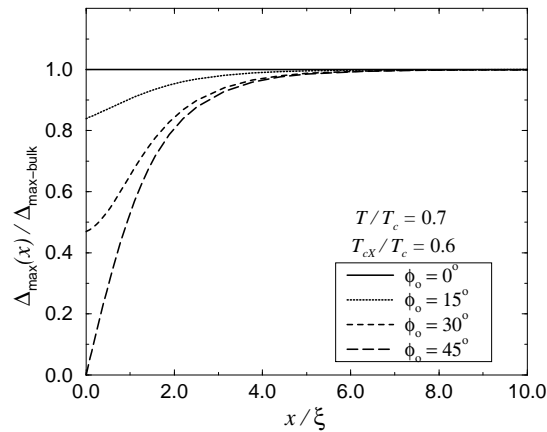


Fig. 8 The maximum of the total order parameter as a function of x in the low coupling constant regime, $T_{cX}/T_c = 0.6$, for various surface to lattice orientation angles, ϕ_o .

The individual gap amplitudes are plotted versus distance from the wall in Figs. 5 and 6 for a temperature $T/T_c = 0.7$. These two graphs portray the behavior of the gap amplitudes for two different coupling constant regimes. For simplicity we have set all of the admixture components to have the same value for T_{cX}/T_c . Note that in both cases the two d -wave components enter with by far the largest amplitudes and are truly the dominant representatives. Indeed, a computation without the s and g -wave components left the amplitudes of the two d -wave components virtually unaltered.

The corresponding maximum gap values are plotted versus distance from the wall in Figs. 7 and 8 and should be compared with Fig. 2 where the admixture is absent. Clearly the system is now able to compensate and avoid (to some degree) gap reduction with the level of compensation being greater for larger T_{cX} . Note that for both transition temperature regimes the total gap maximum for a surface orientation of $\phi_o = 45$ deg is nearly unaltered from the corresponding curve without mixing. This is a special symmetric case whose physics depends strongly on the ratio T/T_{cX} and thus presents a potential mechanism for actually measuring the admixture coupling constants.

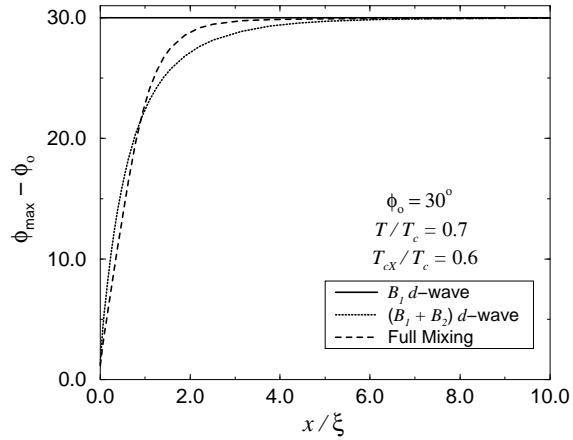


Fig. 9 The angular orientation of the order parameter maximum with respect to the surface normal as a function of x for three different degrees of mixing: a single B_1 d -wave component, a B_1 and a B_2 d -wave component, and *full mixing*.

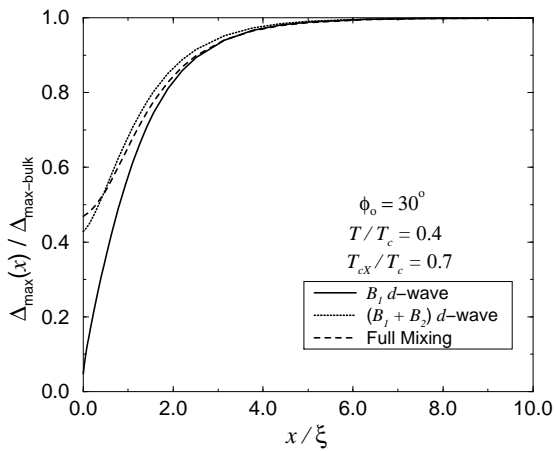


Fig. 10 The maximum of the total order parameter as a function of x for three different degrees of mixing: a single B_1 d -wave component, a B_1 and a B_2 d -wave component, and *full mixing*.

Another striking quality of the self-consistent solution is the complete reorientation of the total gap's nodes toward the optimal configuration (i.e. $\Delta(\phi_{\text{in}}) = \Delta(\bar{\phi}_{\text{out}})$) at the wall, independent of the surface orientation and even for surprisingly small admixture coupling constants. This effect can be plainly seen in Fig. 9 which shows the angular orientation of the maximum of the gap function as a function of x for different degrees of mixing. In the bulk $\phi_{\text{max}} = 0 \text{ deg}, \pm 90 \text{ deg}, \dots$, however in the vicinity of the wall the total gap rotates in an attempt to orient the maximum gap along the surface normal ($\phi_{\text{max}} - \phi_o = 0 \text{ deg}, \pm 90 \text{ deg}, \dots$) at $x = 0$. This overall rotation of the bulk B_1 d -wave gap function is achieved by the mixing in of the B_2 d -wave component. The mixing in of the other components can affect the magnitude and the shape of the total gap function, but they may not bring about an overall rotation. This is presumably the reason for the system's preference of the B_2 d -wave component over the other symmetry components.

The maximum gap values for a given surface orientation are plotted as a function of x in Fig. 10 for various degrees of mixing. Observe that in the immediate vicinity of the wall the addition of the second (B_2) d -wave component has a substantial effect, while the addition of the remaining three has a less pronounced effect. This interpretation is substantiated by the results of the free energy calculations which are plotted in Fig. 4. We display results for a single d -wave component, two d -wave components, and the fully mixed case. Clearly, the inclusion of the A_1 and A_2 components in addition to the B_1 and B_2 components improves the free energy very little. Indeed, the lines lie within a few percent of each other for most surface orientations.

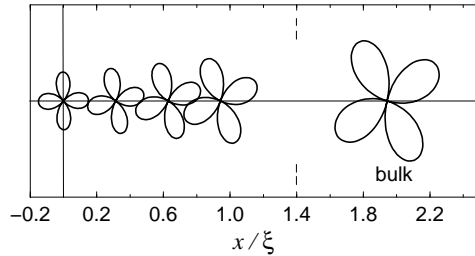


Fig. 11 The orientation and magnitude of the total order parameter as a function of distance from the wall for a surface to lattice orientation angle of $\phi_o = 30 \text{ deg}$. The bulk order parameter (at $x = \infty$) is included for comparison.

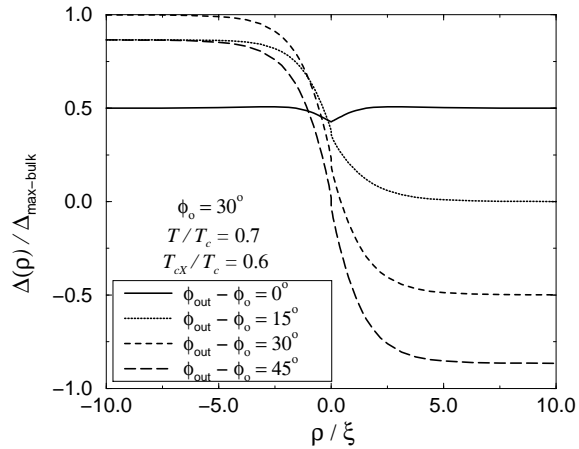


Fig. 12 The local order parameter experienced by a quasiparticle moving along a trajectory of angle ϕ_{out} for a surface to lattice orientation angle of $\phi_o = 30 \text{ deg}$. This is the case of an order parameter consisting of B_1 and B_2 d -wave components. The parameter ρ is the coordinate position along the trajectory and is related to x via $\rho = x / \cos \phi_{\text{out}} - \phi_o$. The point of reflection is taken to be $\rho = 0$.

The crucial importance of the B_2 components is emphasized in Fig. 11, which depicts the angular orientation of the gap function with respect to the surface normal as a function of position. In this figure we consider an order parameter consisting of only the B_1 and B_2 d -wave components. The addition of B_2 allows the system to rotate the total gap maximum toward its optimal orientation (normal to the surface) at the wall. This occurs for both large and small coupling constants and represents one of the most prominent results of this calculation. We fully expect that this could have profound consequences for measurements since even a small admixture assures that the order parameter assumes a symmetric orientation at the wall *regardless* of its bulk orientation.

We conclude our presentation of the numerical results by presenting a plot of the local gap experienced by a quasiparticle along a given trajectory. The results for the $B_1 + B_2$ mix are shown in Fig. 12 and should be compared with Fig. 3. The fact that the total gap has rotated toward its optimal orientation at the wall can be seen, for example, by examining the $\phi_{\text{Out}} - \phi_o = 0$ trajectory where the local gap is now greater at the wall than in the case without mixing (compare with Fig. 3).

IV. CONCLUSIONS

In this paper we have examined the thermodynamic properties of an anisotropically paired superconductor in the vicinity of a perfectly reflecting surface. In particular we considered an order parameter which can be expressed as a linear combination of components transforming as the A_1 , A_2 , B_1 , and B_2 representations of the D_{4h} (tetragonal) group. We carried out self-consistent calculations of the various gap amplitudes within the quasiclassical theory of superconductivity. Such calculations are needed as a starting point for calculations of a number of physically relevant quantities such as the excitation spectrum, the surface impedance, Josephson couplings, etc. Another important example is the tunneling density of states which is discussed in [II].

Starting from the assumption that a d -wave order parameter transforming as the B_1 representation is the bulk stable phase, we showed that even for a small T_{cb_2} the mixing in of a B_2 component can have a profound effect on the order parameter structure near the wall. This arises from the consequent effective rotation of the total gap toward the optimal (i.e. symmetric) orientation in the immediate vicinity of the wall. The effects of the mixing in of the A_1 and A_2 components has a smaller, yet noticeable, influence on the gap function, while their effect on the surface free energy is considerably less. Thus the presence of the A_1 and A_2 symmetries has a minor effect on the thermodynamic properties of the system, but can have a more pronounced effect on the excitation spectrum. The strongest pair-breaking for a B_1 symmetry order parameter is obtained at a 45 deg surface, and for a B_2 order parameter at a surface along one of the crystal axis (0 deg surface). We considered here ideal surfaces without roughness or degradation. This represents the optimal configuration for probing the order parameter by surface measurements. Surface imperfections will wash out, to some degree, the measurable orientational effects of an anisotropic order parameter. As a result, experiments should be performed preferentially at clean and well characterized surfaces oriented perpendicular to the ab -planes.

Note Added in Proof. After the submission of this manuscript we received a preprint by M. Matsumoto and H. Shiba in which the possibility of the mixing in of subdominant symmetry components which break time-reversal symmetry is discussed. We have not allowed for the possibility of such states in our calculations. These time-reversal symmetry breaking states are stable in certain regions of the coupling-constant/temperature parameter space. All of the calculations in the current manuscript, however, were done in a region of parameter space where these time-reversal breaking states are not stable.

ACKNOWLEDGEMENTS

The research of L.J.B was supported by the Fulbright Commission and that of M.P. by the Alexander von Humboldt-Stiftung. D.R. was supported, in part, by the Graduiertenkolleg "Materialien und Phänomene bei sehr tiefen Temperaturen" of the DFG. J.A.S. acknowledges partial support by the Science and Technology Center for Superconductivity through NSF Grant no. 91-20000. Authors D.R. and J.A.S. also acknowledge additional support from the Max-Planck-Gesellschaft and the Alexander von Humboldt-Stiftung.

-
- [1] L. J. Buchholtz and G. Zwirner, Phys. Rev. B **23**, 5788 (1981).
- [2] D. J. Scalapino, Physica C **235-240**, 107 (1994).
- [3] D. Pines, Physica C **235-240**, 113 (1994).
- [4] W. N. Hardy *et al.*, Phys. Rev. Lett. **70**, 3999 (1993).
- [5] D. A. Wollman *et al.*, Phys. Rev. Lett. **71**, 2134 (1993).
- [6] D. A. Brawner and H. R. Ott, Phys. Rev. B **50**, 6530 (1994).
- [7] C. C. Tsuei *et al.*, Phys. Rev. Lett. **73**, 593 (1994).
- [8] J. R. Kirtley *et al.*, Nature **373**, 225 (1995).
- [9] Y. N. Ovchinnikov, Zh. Eksp. Teor. Fiz. **56**, 1590 (1969).
- [10] V. Ambegaokar, P. G. de Gennes, and D. Rainer, Phys. Rev. A **9**, 2676 (1974).
- [11] G. Kieselmann and D. Rainer, Z. Phys. B **52**, 267 (1983).
- [12] W. Zhang, J. Kurkijärvi, and E. Thuneberg, Phys. Lett. **109A**, 238 (1985).
- [13] L. J. Buchholtz, Phys. Rev. B **33**, 1579 (1986).
- [14] N. B. Kopnin, J. Low Temp. Phys. **65**, 433 (1986).
- [15] W. Zhang, J. Kurkijärvi, and E. Thuneberg, Phys. Rev. B **36**, 1987 (1987).
- [16] W. Zhang and J. Kurkijärvi, J. Low Temp. Phys. **73**, 483 (1988).
- [17] L. J. Buchholtz, Phys. Rev. B **44**, 4610 (1991).
- [18] N. B. Kopnin, P. I. Soininen, and M. Salomaa, J. Low Temp. Phys. **85**, 267 (1991).
- [19] N. B. Kopnin and P. I. Soininen, J. Low Temp. Phys. **88**, 199 (1992).
- [20] L. J. Buchholtz, J. Low Temp. Phys. **92**, 43 (1993).
- [21] L. J. Buchholtz, M. Palumbo, D. Rainer, and J. A. Sauls, J. Low Temp. Phys. **101**, (1995).
- [22] G. Volovik and L. P. Gor'kov, JETP Lett. **39**, 674 (1985).
- [23] G. Eilenberger, Z. Phys. **214**, 195 (1968).
- [24] A. I. Larkin and Y. N. Ovchinnikov, Zh. Eksp. Teor. Fiz. **55**, 2262 (1968), [Sov. Phys. JETP **28**, 1200 (1969)].
- [25] A. I. Larkin and Y. N. Ovchinnikov, Zh. Eksp. Teor. Fiz. **68**, 1915 (1975), [Sov. Phys. JETP **41**, 960 (1976)].
- [26] G. Eliashberg, Zh. Eksp. Teor. Fiz. **61**, 1254 (1971), [Sov. Phys. JETP **34**, 668 (1972)].
- [27] U. Eckern and A. Schmid, J. Low Temp. Phys. **45**, 137 (1981).
- [28] J. W. Serene and D. Rainer, Physics Reports **4**, 221 (1983).
- [29] J. Rammer and H. Smith, Rev. Mod. Phys. **58**, 323 (1986).
- [30] A. I. Larkin and Y. N. Ovchinnikov, in *Nonequilibrium Superconductivity*, edited by D. Langenberg and A. Larkin (Elsevier Science Publishers, Holland, 1986), p. 493.
- [31] R. Combescot and J. Labbé, Physica C **153-155**, 204 (1988).
- [32] J. Friedel, J. Phys.: Condensed Matter **1**, 7757 (1989).
- [33] D. M. Newns, C. C. Tsuei, P. C. Pattnaik, and C. L. Kane, Comments Condens. Matter Phys. **15**, 273 (1992).
- [34] R. J. Radtke and M. R. Norman, Phys. Rev. B **50**, 9554 (1994).
- [35] P. W. Anderson, In Proceedings of the U. Miami Workshop on High-Temperature Superconductivity, to be published in J. Supercond. (1995).
- [36] P. Monthoux and D. Pines, Phys. Rev. B **47**, 6069 (1993).
- [37] C.-R. Hu, Phys. Rev. Lett. **72**, 1526 (1994).